

# MAGNETIC MICROSTRUCTURE OF NEAR-SURFACE LAYERS OF EPITAXIAL FILMS OF IRON-YTTRIUM GARNET IMPLANTED BY PHOSPHORUS IONS

V.M. PYLYPIV

V. Stefanyk Ciscarpathian National University

(57, Shevchenko Str., Ivano-Frankivsk 76000, Ukraine; e-mail: mif@pu.if.ua)

UDC 548.73/.75+621

©2008

On the basis of the data of conversion Mössbauer spectroscopy, the process of generation of radiation-induced defects in monocrystalline epitaxial films of iron-yttrium garnet (YIG) irradiated by  $P^+$  ions with an energy of 65 keV and doses of  $5 \times 10^{14}$ ,  $1.8 \times 10^{15}$ , and  $1 \times 10^{16} \text{ cm}^{-2}$  is studied. The mechanisms of disordering of the crystal and magnetic microstructures of an implanted layer are considered. The interconnection of thermostimulated changes of the magnetic microstructure with a transformation of intracrystalline electric fields is studied. The presence of two magnetically nonequivalent positions of  $Fe^{3+}$  ions and paramagnetic  $Fe^{2+}$  ions in the tetrahedral sublattice of the near-surface layer of an YIG film is established. The spatial orientation of the magnetic moments of separate sublattices of iron is calculated. The changes in parameters of the superfine interaction after the implantation and annealing are traced and substantiated.

conditions of the growth and the postgrowth physico-chemical processing, this makes it possible to create magnetic micro- and macrostructures of the required type where the saturation magnetization, constant of uniaxial anisotropy, and parameters of attenuation of magnetostatic waves are changed. The necessity to control the spatial distribution of inhomogeneous magnetic fields induced the need in detailed studies of both a magnetic microstructure of near-surface YIG layers and the influence of conditions of the growth and the processing of films on it on all the stages of preparation.

## 1. Introduction

The interconnection of structural and magnetic properties of epitaxial films with the structure of garnet (in particular, of YIG) and the means of their target modification are studied for three decades, and the wide spectrum of possible practical applications of this material as the active medium of electronic devices stimulates the continuation of the scientific search in this branch. On the initial stage (the 1970-1980s), the main accent was made on the development of film epitaxial structures for the devices of SHF technique and systems of energy-independent magnetic memory; in the 1990s, the interest in film garnet materials was strengthened in connection with the fabrication of planar waveguide structures and lasers. At present time, the main attention is given to the development of active materials for sensor units of visual magnetometry and to the application of the given material in the field of high-frequency transmission and information processing. The presence of three cationic positions of different sizes in YIG, which are coupled by the ferromagnetic interaction, allows one to control the chemical composition in the widest limits. With the simultaneous variation in

## 2. Objects and Method of Studies

The YIG films with nominal composition  $Y_3Fe_5O_{12}$  were grown by the method of liquid-phase epitaxy under industrial conditions on a dielectric nonmagnetic support made of gallium-gadolinium garnet  $Gd_3Ga_5O_{12}$  of about  $500 \mu\text{m}$ . The studied films of  $10.2 \mu\text{m}$  in thickness were oriented in plane (111), the disorientation angle being at most  $7'$ . The supercooling temperature of a solution-melt was  $10^\circ\text{C}$ , and the stability of a temperature mode was held to within  $0.1^\circ\text{C}$ . The surface of specimens was etched in orthophosphoric acid at a temperature of  $130^\circ\text{C}$  to remove the inhomogeneous "film-air" layer of 10–15 nm in thickness. The specimens were irradiated by phosphorus ions with an energy of 65 keV and doses of  $5 \times 10^{14}$ ,  $1.8 \times 10^{15}$ , and  $1 \times 10^{16} \text{ cm}^{-2}$ . The implantation was carried out at room temperature on an installation of the "Vezuvii" type in the mode excluding the effect of channeling. To avoid the effect of self-annealing, the implantation current density was at most  $2 \mu\text{A}/\text{cm}^2$ . After the implantation, the specimens underwent the isothermal annealing in the flow of oxygen at a temperature of  $950^\circ\text{C}$  for 300 min.

The crystalline structure of YIG belongs to the cubic space group Ia3d, and the elementary cell contains 16 crystallographically equivalent ions of Fe in octacoordinated ( $a$ ) voids with the point symmetry  $\bar{3}$  and

24 equivalent ions of Fe in tetracoordinated ( $d$ ) voids with the point symmetry  $\bar{4}$ . The point groups for the  $a$ - and  $d$ -positions of Fe define the axial symmetry of the tensors of the gradients of intracrystalline electric fields (GEF), whose symmetry axes coincide, respectively, with the crystallographical directions  $\{111\}$  and  $\{100\}$ . The magnetic ordering in the structure of IYG is defined by both the electrostatic fields induced into the nuclei of Fe ions of the lattice and the intrinsic electron shells with a non centrally symmetric distribution of the charge. The antiferromagnetic ordering in IYG appears as a result of the mediate interaction between Fe ions through ions of oxygen. According to [1], the magnetic moments of  $\text{Fe}^{3+}$  are as follows:  $m_{24d} = 4.2\mu_B$  and  $m_{16a} = -4.0\mu_B$ . The total magnetic moment of each domain of a film is directed along an axis of the  $\langle 111 \rangle$  type which is the axis of easy magnetization [2].

The characteristic feature of IYG consists in the simultaneous presence of the electric quadrupole and magnetic dipole interactions with approximately identical intensities, which creates certain difficulties in the mathematical treatment of experimental data. For epitaxial films  $\text{Y}_3\text{Fe}_5\text{O}_{12}$ , the additional active factor is presented by the surface of a ferrimagnetic specimen. A jump of the magnetization on this surface induces the appearance of the additional planar component of the magnetization. The effect of surface demagnetization causes a turn of the axis of easy magnetization from the direction along a normal to a direction lying in the film plane.

In order to study the magnetic microstructure, the method of conversion electron Mössbauer (CEM) spectroscopy was used. A spectrometer of the YaGRS-4M type operated in the mode of steady accelerations. To improve the quality of the CEM spectra of iron, oxide  $\text{Fe}_2\text{O}_3$  enriched by isotope  $\text{Fe}^{57}$  up to 8% was added to the initial charge. The CEM spectra of  $\text{Fe}^{57}$  were obtained at room temperature with the use of a source of gamma-quanta,  $\text{Co}^{57}$ , in the Cr matrix with an activity of  $\sim 30 \mu\text{Ci}$ . Conversion electrons were registered with a proportional gas-flow counter containing a mixture of 96% He + 4%  $\text{CH}_4$ . The calibration of the CEM spectra of iron was performed relative to metallic  $\alpha$ -Fe.

The Mössbauer spectroscopy allows one to separate the contributions of individual groups of Fe ions with different values of the angle  $\theta$  between the directions of GEF and the vector of their total magnetic moment that is parallel to the direction of the effective magnetic field  $H_{\text{eff}}$  on the nuclei of these ions. In the general case, the Mössbauer spectrum of IYG is a superposition of seven partial sextets. For monocrystalline films of  $\text{Y}_3\text{Fe}_5\text{O}_{12}$

with the orientation in plane (111), the collection of angles is reduced to three ones ( $\theta_{\alpha_1} = 0$ ,  $\theta_{\alpha_2} = 70^\circ 52'$ , and  $\theta_d = 54^\circ 44'$ ), and the spectrum can be approximated by three components with the ratios of integral intensities  $S_d : S_{\alpha_1} : S_{\alpha_2} = d : \alpha_1 : \alpha_2$ . On the ionic implantation, the initial stages of the accumulation of a dose are characterized by the processes of radiation-induced disordering: a symmetry of the local environment of atoms in the crystal lattice is distorted, the electron density is redistributed, and the geometry of the exchange bond  $\text{Fe}_a\text{-O-Fe}_d$  is violated. An increase in the radiation dose leads to the accumulation of radiation-induced defects, the overlapping of certain cascades of atom-atom collisions, and the appearance of radiation-disordered regions. The main purpose of the present work is the experimental determination of changes of a spatial orientation of the magnetic moments of crystallographically nonequivalent ions of iron after the implantation of P ions and the following annealing.

### 3. Experimental Results and Their Discussion

The character of changes in a magnetic ordering in the near-surface layer of an IYG film was studied with the use of the method of Mössbauer spectroscopy of conversion electrons (CEM-spectroscopy). This method allows one to obtain the information about changes in a symmetry of the nearest environment of nuclei of Fe in the near-surface layer of a film of  $\leq 100$  nm in thickness after the implantation and annealing. In the general case in the analysis of experimental Mössbauer spectra, it is necessary to use the Hamiltonian of mixed superfine interaction with regard for the simultaneous existence of the magnetic dipole and electric quadrupole splittings of the superfine structure of spectra. The diagonalization of the matrix of the Hamiltonian for nuclei was performed according to the method proposed in [6]. The partial sextets were assumed to be a superposition of Lorentzians. The coordinate system was chosen so that the tensor of GEF was diagonal, and the  $z$  axis was parallel to  $U_{zz}$ . In the used model, the tensor of GEF was assumed to be axially symmetric, and the parameter of asymmetry

$$\eta = \frac{U_{xx} - U_{yy}}{U_{zz}} = 0.$$

Based on the crystallographic preconditions, the experimental spectrum was expected to have the form of a superposition of three partial sextets, but the eligible result of the approximation was obtained only after the introduction of two magnetically nonequivalent  $d$ -posi-

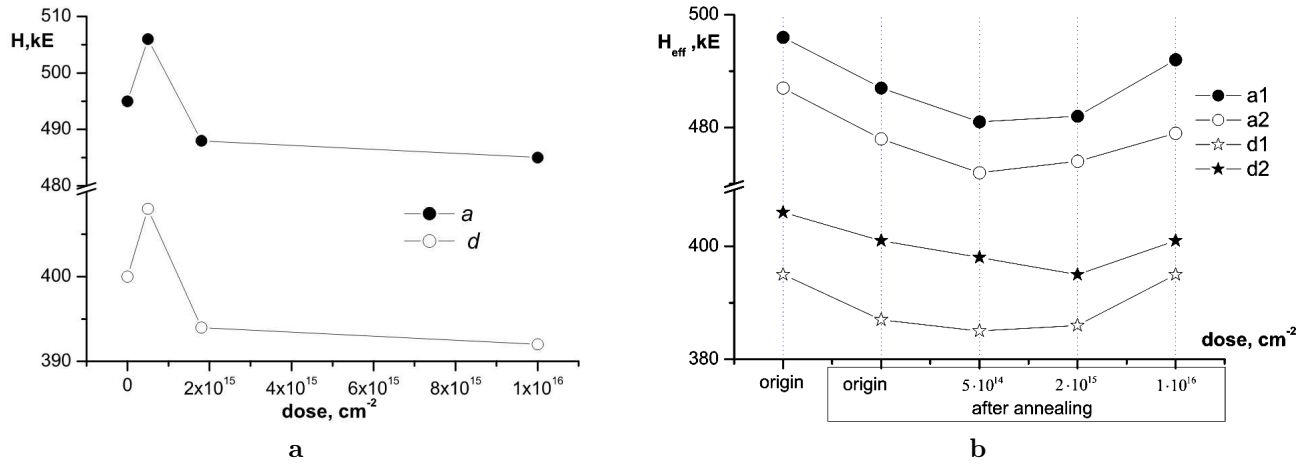


Fig. 1. Effective magnetic fields  $H_{\text{eff}}$  on the nuclei of  $\text{Fe}^{57}$  ions in the  $a$ - and  $d$ -positions versus the dose of irradiation of IYG films: (a) after the implantation; (b) after the implantation and annealing

tions with different values of effective magnetic fields on nuclei  $\text{Fe}^{57}$  and other paramagnetic parameters (isomeric shift, magnetic field  $H_{\text{eff}}$ , and axial component of GEF  $U_{zz}$ ). An analogous result was obtained in [3] and interpreted as a consequence of the violation of anionic stoichiometry due to both the nonequilibrium process of growth of a film and the introduction of extrinsic atoms into the structure of garnet from the solution-melt on the final stages of the epitaxy. At the same time, the breaking of a crystal structure under ionic implantation leads to the appearance of a number of magnetically nonequivalent positions of iron with reduced effective fields on nuclei up to the origination of the paramagnetic state of Fe ions. Taking these facts into account, only the  $a$ - and  $d$ -positions of Fe were separated on the decoding of Mössbauer spectra after the implantation.

**Table 1. Parameters of partial components of the CEM spectra of an IYG film after the implantation**

Dose, $\text{cm}^{-2}$	Crystallographic position	$\Delta_s$ , mm/s	$H$ , kOe	$\delta_s$ , mm/s	$\omega$ , mm/s	$S$ , %
Init.	$a$	0.10	495	0.63	0.40	33.2
	$d$	0.05	400	0.34	0.57	62.9
	$D$	2.40	–	0.48	0.53	3.9
$5 \times 10^{14}$	$a$	0.13	506	0.69	0.47	17.3
	$d$	0.01	408	0.47	0.68	35.4
	$D$	1.17	–	0.61	0.59	47.3
$1.8 \times 10^{15}$	$a$	0.09	488	0.73	0.65	17.3
	$d$	0.01	394	0.44	0.56	33.3
	$D$	1.22	–	0.55	0.58	49.4
$1 \times 10^{16}$	$a$	0.12	485	0.64	0.43	14.5
	$d$	–0.02	392	0.42	0.66	29.7
	$B$	1.01	–	0.59	0.66	55.8
Error		$\pm 0.03$	$\pm 3$	$\pm 0.04$	$\pm 0.03$	$\pm 0.3$

The results of calculations of the CEM spectra of the initial specimen decoded with regard for the presence of two pairs of magnetically nonequivalent  $a$ - and  $d$ -positions and with the separation of only the  $a$ - and  $d$ -positions of Fe, as well as the typical spectrum of an implanted specimen ( $D = 1 \times 10^{16} \text{ cm}^{-2}$ ) before and after the annealing, are given in Tables 1 and 2. In what follows, the dynamics of changes in the magnetic microstructure after the annealing is traced separately for specimens implanted and specimens annealed after the implantation, with the use of different approximations of the spectrum of the initial specimen.

It is revealed that the dose dependence of effective magnetic fields  $H_{\text{eff}}$  on the nuclei of Fe ions in the  $a$ - and  $d$ -positions of specimens after the implantation is characterized by a local maximum at the minimum dose of implantation (Fig. 1, *a*). A similar effect was observed in work [4]. Changes in  $H_{\text{eff}}$  are caused by the deformation-induced redistribution of the spin density of electrons of the  $s$ -shell of atom  $\text{Fe}^{57}$ . On the initial stage of the formation of radiation-disordered regions (the implantation dose was equal to  $5 \times 10^{14} \text{ cm}^{-2}$ ), the implantation induces local variations in the interplane distance: there appear the tensile stress in the direction normal to the film plane and the compressive stress in the parallel direction. At the same time, the isomeric shifts increase (Fig. 2, *a*), which testifies to the decrease in the degree of covalency of the chemical bond  $\text{Fe-O}$  and is explained by the increase in the range of the exchange interaction and a change of the environment of Fe atoms, a decrease in the overlapping of the electron shells of  $\text{Fe}^{3+}$  and  $\text{O}^{2-}$ , and, as a result, the localization of the wave function of  $4s$ -electrons on nucleus  $\text{Fe}^{57}$ .

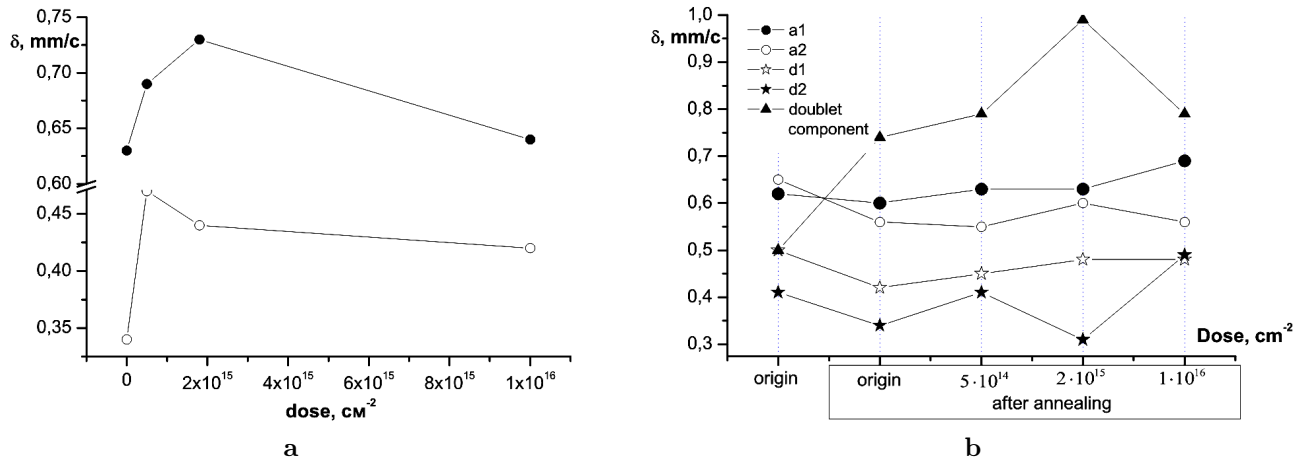


Fig. 2. Isomeric shift in the Mössbauer spectra of IYG films versus the dose of irradiation of the nuclei of Fe ions: (a) in the  $a$ - and  $d$ -sublattices after the implantation; (b) in the  $a$ - and  $d$ -sublattices and the doublet component of the spectrum after the implantation and the following annealing

The increase in the dose leads to both the joining of separate amorphous paramagnetic clusters of  $\sim 0.1 \text{ nm}^3$  in size (in the modeling, the processes of annihilation and the possibility for the cascades of secondary collisions to overlap were not considered) and the formation of extended magnetically disordered regions with linear

sizes of  $\sim 10 \text{ nm}$ . The increase in the implantation dose leads to a sharp decrease in the effective magnetic fields  $H_{\text{eff}}$  on the nuclei of Fe ions in the  $a$ - and  $d$ -positions, which is due to the fracture of both the crystal lattice and, respectively, the exchange bonds Fe–O.

Table 2. Parameters of partial components of the CEM spectra of an IYG film after the implantation and annealing

Dose, $\text{cm}^{-2}$	Crystallographic position	$\beta^\circ$	$\bar{\beta}_a, \bar{\beta}_d$	$U_{zz} \times 10^{21}$ , $\text{W/m}^2$	$H$ , kOe	$\delta_s$ , mm/s	$\omega$ , mm/s	$S$ , %
Initial	$a_1$	63.6	73.4	1.05	496	0.62	0.33	27.5
	$a_2$	104.3	73.4	3.05	487	0.65	0.33	9.2
	$d_1$	77.9	78.4	-2.10	395	0.50	0.41	34.5
	$d_2$	78.9	78.4	-5.23	406	0.41	0.37	26.0
	$D$					0.50	0.33	2.8
Initial annealed	$a_1$	74.2	83.1	1.22	487	0.60	0.37	27.8
	$a_2$	110.7	83.1	3.22	478	0.56	0.36	9.3
	$d_1$	72.9	77.05	-5.16	387	0.42	0.44	28.70
	$d_2$	82.1	77.05	4.02	401	0.34	0.44	32.0
	$D$					0.74	0.34	2.2
$5 \times 10^{14}$	$a_1$	76.3	83.2	0.87	481	0.63	0.36	27.8
	$a_2$	104.3	83.2	2.87	472	0.55	0.36	8.9
	$d_1$	70.6	75.4	-5.22	385	0.49	0.45	34.3
	$d_2$	80.3	75.4	6.42	398	0.33	0.41	26.5
	$D$					0.79	0.36	2.5
$1.8 \times 10^{15}$	$a_1$	74.59	82.8	0.91	482	0.63	0.32	27.9
	$a_2$	108.2	82.8	2.92	474	0.60	0.32	9.3
	$d_1$	82.9	81.05	-0.27	386	0.48	0.40	31.0
	$d_2$	79.2	81.05	5.37	395	0.31	0.36	30.4
	$D$					0.99	0.32	1.4
$1 \times 10^{16}$	$a_1$	74.7	78.5	0.68	492	0.69	0.47	28.4
	$a_2$	90.0	78.5	2.68	479	0.56	0.47	9.5
	$d_1$	79.6	83.5	-6.96	395	0.48	0.47	27.7
	$d_2$	87.4	83.5	5.40	401	0.49	0.43	30.8
	$D$					0.79	0.48	3.6
Error		$\pm 1.0$	$\pm 1.0$	$\pm 0.09$	$\pm 3.0$	$\pm 0.03$	$\pm 0.02$	$\pm 0.1$

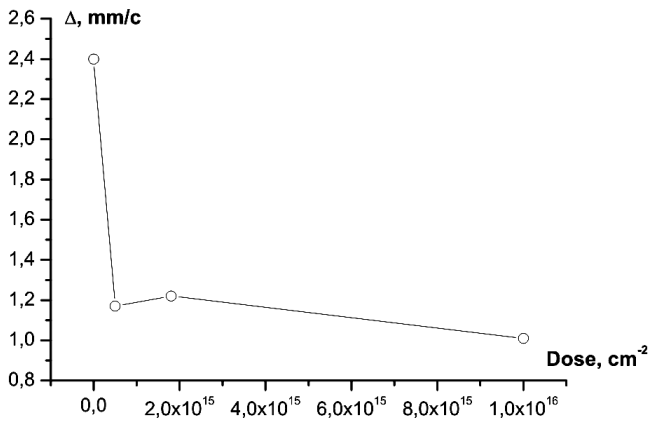


Fig. 3. Value of quadrupole splitting of the doublet component of a spectrum versus the dose of irradiation of IYG films after the implantation

The distortion and the breaking of a symmetry of the nearest environment of Fe atoms on the implantation are revealed on the dose dependence on the quadrupole splitting of the doublet component of a spectrum (Fig. 3). It is obtained that the quadrupole splitting has tendency to decrease with increase in the radiation dose. This indicates the growth of the relative content of  $\text{Fe}^{3+}$  ions in a high-spin state or  $\text{Fe}^{2+}$  ions in a low-spin state, which is confirmed by the values of isomeric shifts of the doublet component. However, the separation the contributions of ions in certain states by considering the change of the covalency of a chemical bond and the distortion of the crystalline and valent gradients of electric fields induced on nucleus  $\text{Fe}^{57}$  cannot be performed. For a nonimplanted specimen, the decoding by both methods fixed the presence of the doublet component observed also in [5]; according to the value of quadrupole splitting, the doublet is unambiguously associated with  $\text{Fe}^{2+}$  ions in the paramagnetic state. A reason for both a change in the valency and the elimination of Fe ions from the superexchange interaction is their substitution by nonmagnetic  $\text{Pb}^{2+}$ ,  $\text{Pb}^{4+}$ , and  $\text{Pt}^{4+}$  ions. It is known [6] that  $\text{Pb}^{2+}$  and  $\text{Pb}^{4+}$  ions occupy octahedral positions by displacing  $\text{Fe}^{3+}$  with probabilities of 0.4 and 0.3, respectively, whereas  $\text{Pt}^{4+}$  ions occupy exclusively octapositions. The fact that Fe ions in the paramagnetic state belong to the tetrasublattice is confirmed by experimental values of the ratio of the integral intensities of subspectra of Fe in octa- and tetravoids of the initial specimen before and after the annealing. The ratio of the populations of  $a$ - and  $d$ -sites of Fe cations in the IYG-structure has the

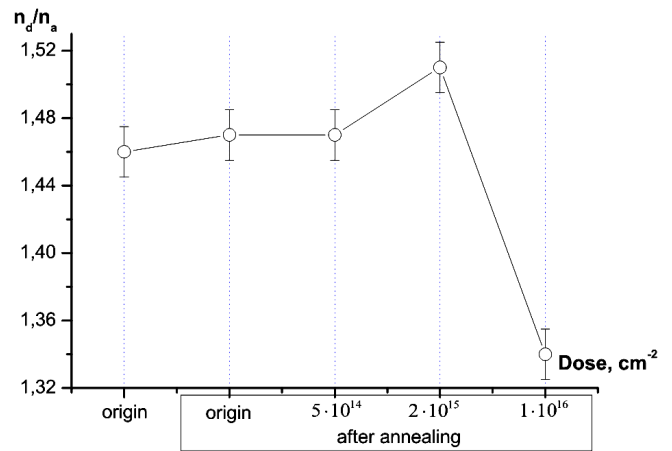


Fig. 4. Change of the relative population of the  $a$ - and  $d$ -sublattices of Fe ions after the implantation and annealing of IYG films

form [7]

$$\frac{n_d}{n_a} = \frac{S_d f_a}{S_a f_d},$$

where  $S_a$  and  $S_d$  are the integral intensities of the corresponding partial subspectra, and  $f_a$  and  $f_d$  are the probabilities of the Mössbauer effect for the octa- and tetrapositions, respectively. The ratio of  $f$ -factors for Fe cations in the  $a$ - and  $d$ -positions in IYG is independent of the degree of substitution of Fe ions and is equal to  $0.94 \pm 0.02$  at room temperature. The changes of populations of the  $a$ - and  $d$ -voids of Fe cations after the implantation and the following annealing are presented in Fig. 4.

Despite the experiment error, it is possible to trace the tendency to the renewal of a magnetic ordering of the annealed IYG film at the implantation doses less than  $1 \times 10^{16} \text{ cm}^{-2}$ . After the annealing of a film implanted with a dose of  $1.8 \times 10^{15} \text{ cm}^{-2}$ , the ratio  $n_d/n_a$  becomes equal to  $1.510 \pm 0.015$ , which testifies the uniformity of the distribution of extrinsic ions of Pb and Pt in the near-surface layer of the film over the cationic sublattices after the ion mixing. However, the implantation dose of  $1 \times 10^{16} \text{ cm}^{-2}$  leads to the unrestored (for the given annealing temperature) processes of crystalline and, respectively, magnetic orderings, which is reflected in a reduction of the ratio of the populations of the  $a$ - and  $d$ -sublattices to  $1.340 \pm 0.015$ . This value confirms one more the fact mentioned in [8] that the tetrahedral cationic sublattice has comparatively greater radiation resistance, which is related to the smaller number of oxygen anions in the first coordination sphere. Changes

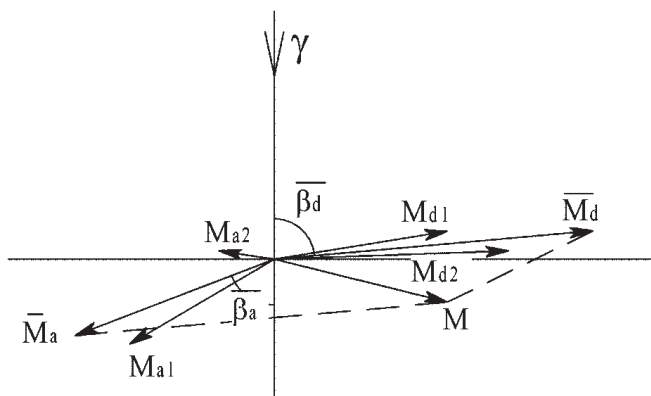


Fig. 5. Spatial orientation of the magnetic moments of Fe atoms in separate sublattices and the total magnetic moment relative to the wave vector of a  $\gamma$ -ray

in the nearest environment and the processes of reconstruction of the crystal structure of implanted films after the annealing cause the changes in the integral effective magnetic fields  $H_{\text{eff}}$  on the nuclei of Fe ions that are placed in different coordinate positions (Fig. 1, *b*).

The effective fields  $H_{\text{eff}}$  for the annealed initial specimen and the specimens implanted at doses up to  $1 \times 10^{16} \text{ cm}^{-2}$  are less than those in the initial specimen and manifest the tendency to a decrease with increase in the implantation dose. The coordinated change in  $H_{\text{eff}}$  is fixed for all sublattices of iron in the annealed specimens, which can be explained by the value of annealing temperature (900 °C), at which both the anionic (up to 400 °C) and cationic (700–900 °C) geometries are restored [9]. The annealing of the initial specimen induces a decrease in isomeric shifts for all positions (Table 2), which can be explained by the temperature-stimulated relaxation of a stressed state of the epitaxial structure and the increase in the degree of covalency of the chemical bond Fe–O [10]. The tendency to the increase in the isomeric shift for different crystallographic positions of nuclei  $\text{Fe}^{57}$  of the annealed specimens can indicate a decrease in the renewal efficiency of the lattice with increase in the implantation dose and with decrease in the overlapping of the electron shells of  $\text{Fe}^{3+}$  and  $\text{O}^{2-}$  ions. The behavior of the isomeric shift for  $\text{Fe}^{2+}$  ions in the tetrasublattices of films after the implantation and annealing is analogous (Fig. 2, *b*). The vector of magnetization of an epitaxial film of IYG lies practically in its plane, which is a result of the effects of demagnetization of the surface [11]. According to [12], the angle between the vector of magnetization and the normal to the surface of an IYG film is equal to  $(71 \pm 5)^\circ$ . The orientation of the vector of magnetization is determined by the competitive manifestation of the

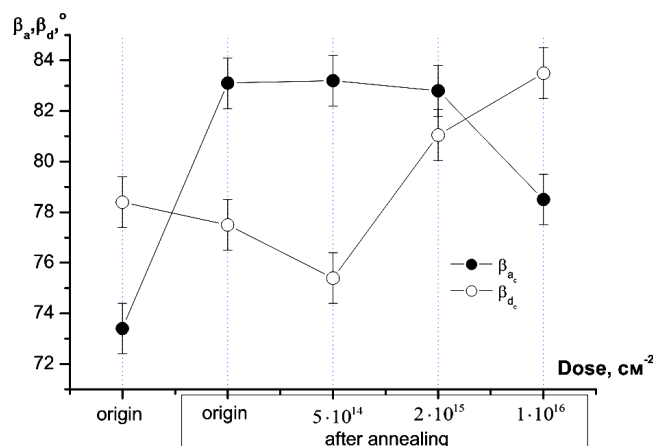


Fig. 6. Change of the polar angles of the orientation of the averaged vectors of the magnetic moments of the *a*- and *d*-sublattices of iron relative to the propagation direction of the beam of  $\gamma$ -rays in IYG films after the implantation and annealing

uniaxial, cubic, and rhombic components of the anisotropy. In the present work, the experimental determination of the polar angles characterizing the orientation of the vectors of magnetic moments of separate Fe sublattices, which are nonequivalent as for their crystal structure, relative to the propagation direction of the beam of  $\gamma$ -rays is realized (the scheme is given in Fig. 5, and the results are presented in Table 2).

The results of the averaging of magnetic moments for Fe ions in the octa- and tetrahedral environment with regard for the experimental populations of separate sublattices are given in Fig. 6. The magnetic moments of ions of sublattices are close to those in the collinear state and are deviated from the normal to the film plane by the same angle, which can be explained by the dominant contribution of the cubic component of the anisotropy. The observed noncollinearity of magnetic moments of the *a*- and *d*-sublattices can be related to the entry of extrinsic atoms in chains with the superexchange interaction on the stage of the epitaxial growth of a film [13] and in the process of reconstruction of the radiation-mixed distorted layer. The annealing of the initial specimen causes the remarkable changes in the orientation of the magnetic moment of the octasublattice, by inducing its turn in the direction of the film plane. It can be assumed that the elimination of growth defects on the annealing and the relaxation of a heterostructure with both the simultaneous redistribution of the basic (Fe, Y) and extrinsic (Pb, Pt) cations and changes in a symmetry of the environment of oxygen influence the value of

uniaxial anisotropy. The last quantity is determined by the population of dodecahedral sites, which are nonequivalent relative to the growth direction of a crystal on the support oriented in plane (111), by extrinsic ions of two different types [12]. For the annealed specimen implanted with a dose of  $1.8 \times 10^{15} \text{ cm}^{-2}$ , the noncollinearity of magnetic moments of the  $a$ - and  $d$ -sublattices disappears in the limits of the measurement error, which correlates with the calculated values of populations of the sublattices (Fig. 1,  $a$ ) and is the evidence of the equilibrium of a crystallographic ordering of the near-surface layer of an IYG film. However, for a given specimen, the maximum divergence in the values of  $|U_{zz}|$  of GEF is observed for the crystallographic positions  $a_1$  and  $a_2$  (Table 1). It is known [14] that the GEF on the nucleus of a Mössbauer atom is created by both ions of the crystal lattice (“crystalline” GEF) and nonspherical valence shells of the Mössbauer atom itself (“valence” GEF). For IYG, the principal role in the electron-nucleus interactions (the formation of effective magnetic fields on nuclei) is played by the contact Fermi-component that is defined by both the density of  $s$ -electrons on nucleus  $\text{Fe}^{57}$  and a degree of their spin polarization as a result of the exchange interaction with  $3d$ -electrons [15]. Even the insignificant changes in a symmetry and a type of the environment of a Mössbauer nucleus essentially affect the degree of covalency of a chemical bond, by deforming the distribution of electron density in the exchange chain  $\text{Fe}_a\text{--O--Fe}_d$ . It is clear that the appearance of the “valence” component of GEF and the dependence of the absolute values of components of the “crystalline” GEF on the structural disorder render the defining influence on the experimental values of  $|U_{zz}|$  (Table 2). On the basis of the data of X-ray diffraction analysis on the coordinates of atoms in the ideal structure of IYG [16], the components  $|U_{zz}|$  of “crystalline” GEF are calculated. For the crystallographic directions  $\{111\}$  and  $\{100\}$  of a cluster formed by 4480 atoms, they are, respectively,  $1.7 \times 10^{21}$  and  $2.9 \times 10^{21} \text{ W/m}^2$  (mean values). The comparison of the calculated values with experimental ones (Table 1) is difficult, because it is impossible to numerically determine the effect of both the “valence” component and structural defects, but it is worth noting the qualitative coincidence  $(|U_{zz}|)_d > (|U_{zz}|)_a$ .

#### 4. Conclusions

1. In a nonimplanted specimen, the doublet component corresponding to  $\text{Fe}^{2+}$  in the paramagnetic state is

discovered; the probable reason for a change of valency and the elimination of Fe ions from the superexchange interaction is their substitution by nonmagnetic  $\text{Pb}^{2+}$ ,  $\text{Pb}^{4+}$ , and  $\text{Pt}^{4+}$  ions during the growth.

2. The deformation-induced changes in both the effective magnetic field on nuclei  $H_{\text{eff}}$  and isomeric shifts in implanted specimens are detected; this testifies to a decrease in the degree of covalency of the chemical bond Fe–O and is explained by both an increase in the range of exchange interaction and a change in the environment of Fe atoms.

3. The presence of two magnetically nonequivalent positions for  $\text{Fe}^{3+}$  which occupy tetrahedral sites is established; this is caused by violations of the anionic stoichiometry due to both the nonequilibrium of the process of growth of a film and the entry of extrinsic atoms from the solution-melt into the structure of garnet on the final stages of the epitaxy.

4. The annealing of a nonimplanted specimen causes a decrease in isomeric shifts for all positions, which is explained by both the temperature-stimulated relaxation of a stressed state of the epitaxial structure and an enhancement of the degree of covalency of the chemical bond Fe–O; the tendency to the increase in isomeric shifts for all positions of annealed implanted specimens is defined by the increase in a distortion of the symmetries of the octahedral and tetrahedral environments of iron and a decrease in the degree of overlapping of the electron shells of  $\text{Fe}^{3+}$  and  $\text{O}^{2-}$ .

5. The observed correlated change in  $H_{\text{eff}}$  for all sublattices of iron of the annealed specimens is explained by the value of annealing temperature ( $900 \text{ }^\circ\text{C}$ ), at which the anionic and cationic geometries are restored.

6. The magnetic moments of Fe ions in the  $a$ - and  $d$ - sublattices are close to those in the collinear state and are deviated from the normal to the film plane by the same angle; the registered noncollinearity is explained by the entry of extrinsic atoms in chains with the superexchange interaction on the stage of epitaxial growth of a film and in the process of reconstruction of the radiation-mixed distorted layer.

1. S. Krupicka, *Physik der Ferrite und der Verwandten Magnetischen Oxide* (Acad. Verlag, Prague, 1973).
2. S.B. Ubizskii, *J. Magn. Magn. Mat.* **195**, 575 (1999).
3. B.K. Ostafiichuk, V.D. Fedoriv, V.O. Kotsyubyns'kyi, and V.V. Moklyak, *Fiz. Khim. Tverd. Tela* **6**, 60 (2005).
4. B.K. Ostafiichuk, L.S. Yablon', and V.O. Kotsyubyns'kyi, *Fiz. Khim. Tverd. Tela* **5**, (744 (2004).
5. V.G. Kostishyn, V.V. Medved', and L.M. Letyuk, *J. Magn. Magn. Mat.* **196**, 215 (2000).

6. R.W. Grant, in *Mössbauer Spectroscopy*, edited by U. Gonser (Springer, Berlin, 1975).
7. A.S. Kamzin and Yu.N. Mal'tsev, *Fiz. Tverd. Tela* **39**, 1248 (1997).
8. B.K. Ostafiichuk, V.A. Oleiunik, V.M. Pylypiv, B.T. Semen, L.M. Smerklo, B.I. Yavorskii, V.I. Kravets, and I.V. Koval', Preprint of the Inst. of Metal Physics of the NASU, No. 1.91 (Kyiv, 1991).
9. V.O. Kotsyubyns'kyi, V.V. Nemoshkalenko, B.K. Ostafiichuk, Ya.P. Salii, V.D. Fedoriv, and P.I. Yurchyshyn, *Metallofiz. Nov. Tekhn.* **23**, 1455 (2001).
10. B.K. Ostafiichuk, O.M. Tkachuk, V.M. Tkachuk, and V.D. Fedoriv, *Zh. Fiz. Dosl.* **3**, 113 (1999).
11. S.V. Vonsovskii, *Magnetism* (Nauka, Moscow, 1971) (in Russian).
12. G. Balestrino, S. Lagomarsino, B. Maturi, and A. Tucciarone, *IEEE Trans. Magn.* **20**, 1864 (1984).
13. M.A. Gilleo, in *Ferromagnetic Insulators: Garnets-Ferromagnetic Materials*, edited by E.P. Wohlfarth (North-Holland, Amsterdam, 1980), Vol.2, pp.1-53.
14. P.P. Seregin, *Physica. Physical Foundations of Mössbauer Spectroscopy* (Publish. House of St.PPTU, St.-Petersburg, 2002) (in Russian).
15. H. Winkler and R. Eisberg, E. Alp, R. Ruffer *et al.*, *Z. Phys. B: Cond. Matter* **49**, 331 (1983).
16. V.I. Kravets', Ph.D. Thesis, Inst. of Metal Physics of the NASU, Kyiv (1998).

Received 20.06.07.

Translated from Ukrainian by V.V. Kukhtin

МАГНІТНА МІКРОСТРУКТУРА ПРИПОВЕРХНЕВИХ ШАРІВ ЕПІТАКСІЙНИХ ПЛІВОК ЗАЛІЗО-ІТРІЄВОГО ГРАНАТУ, ІМПЛАНТОВАНИХ ІОНАМИ ФОСФОРУ

В.М. Пилипів

Резюме

На основі даних конверсійної мессбауерівської спектроскопії досліджено процес генерації радіаційних дефектів у монокристалічних епітаксійних плівках залізо-ітрієвого гранату (ЗІГ), опромінених іонами  $P^{+}$  з енергією 65 кеВ та дозами  $5 \cdot 10^{14}$ ;  $1,8 \cdot 10^{15}$  і  $1 \cdot 10^{16}$   $cm^{-2}$ . Розглянуто механізми розупорядкування кристалічної і магнітної мікроструктури імпантованого шару. Досліджено взаємозв'язок термостимульованих змін магнітної мікроструктури з трансформацією внутрішньокристалічних електричних полів. Встановлено наявність у тетраедричній підґратці приповерхневого шару плівки ЗІГ двох магнітонеєквівалентних позицій іонів  $Fe^{3+}$  та парамагнітних іонів  $Fe^{2+}$ . Розраховано просторову орієнтацію магнітних моментів окремих підґраток заліза. Простежено та обґрунтовано зміни значень параметрів надтонкої взаємодії після імплантації та відпаалу.